Main sequence stars as calibrators for interferometry

Pierre Kervella[a,b], Frédéric Thévenin[c], Damien Ségransan[d] and Emmanuel Di Folco[e]

[a] LESIA, UMR 8109, Observatoire de Paris-Meudon, F-92195 Meudon Cedex, France;
[b] European Southern Observatory, Alonso de Cordova 3107, Vitacura, Santiago, Chile;
[c] Observatoire de la Côte d'Azur, BP 4229, F-06304 Nice Cedex 4, France;
[d] Observatoire de Genève, CH-1290 Sauverny, Switzerland;
[e] European Southern Observatory, Karl-Schwarzschildstr. 2, D-85748 Garching, Germany.

ABSTRACT

We present in this paper new and accurate calibrations of the surface brightness-color relations that can be used to predict accurately the angular diameter of dwarf stars and subgiants. These stars present significant advantages as calibrators for interferometric observations. In many cases, they are more stable than giants and supergiants, as they are steadily burning their hydrogen. They are present in large numbers in the solar neighborhood, and offer a broad variety of colors. Their proximity allows to minimize the problems related to interstellar extinction in estimating their true magnitudes and colors. Excluding multiple stars, fast rotators and highly variable stars, it is possible to select reliable calibrators from spectro-photometric observations. Moreover, as opposed to the giant and supergiant stars, the photospheric diameter of dwarf stars is well defined and less sensitive to the assumed atmosphere models. In particular, the limb darkening related problems are alleviated at infrared wavelengths.

Keywords: interferometry, calibrators, surface brightness

1. INTRODUCTION

Interferometric measurements rely on the calibration of the instrumental interferometric transfer function using stars of known angular sizes, usually refered to as calibrators. In this process, the precision of the *a priori* estimate of the angular diameters of these stars is potentially an important source of systematic uncertainty on the measurement of the scientific target. While it has historically been possible to avoid this question by choosing faint and mostly unresolved calibrators, the new interferometers with baseline lengths of several hectometers and operating at short wavelengths will not be able to obtain fringes on "unresolved" stars (due to their faintness). In order to maintain the systematic errors at a low level, it is therefore essential to calibrate new tools to predict the angular diameters of calibrator stars with high accuracy.

The surface brightness relations (hereafter SB) link the emerging flux per solid angle unit of a light-emitting body to its color (or effective temperature). These relations are of considerable astrophysical interest, as a well-defined relation between a particular color index and the surface brightness can provide accurate predictions of the stellar angular diameters. Such predictions are essential for the calibration of long-baseline interferometric observations.

We propose in the present paper new and accurate calibrations of the SB-color relations of dwarfs and subgiants based on direct interferometric measurements of nearby members of these two luminosity classes. The range of validity of these relations is very wide, from spectral type A0 to M2 in the case of dwarfs, and between A0 and K0 for subgiants. Our primary purpose is to establish reliable relations that can be used to predict the angular size of calibrators for long baseline interferometry.

Send correspondence to P.K.: E-mail: pierre.kervella@obspm.fr

2. CALIBRATION OF THE SURFACE BRIGHTNESS-COLOR RELATIONS

2.1. Direct and inverse surface brightness relations

By definition, the bolometric surface flux $f \sim L/D^2$ is linearly proportional to T_{eff}^4, where L is the bolometric flux of the star, D its bolometric diameter and T_{eff} its effective temperature. In consequence, $F = \log f$ is a linear function of the stellar color indices, expressed in magnitudes (logarithmic scale), and SB relations can be fitted using (for example) the following expressions:

$$F_B = a_0 \, (B - V)_0 + b_0 \tag{1}$$

$$F_V = a_1 \, (V - K)_0 + b_1 \tag{2}$$

$$F_H = a_2 \, (B - H)_0 + b_2 \tag{3}$$

where F_λ is the surface brightness. When considering a perfect blackbody curve, any color can in principle be used to obtain the SB. The index 0 designates the dereddened magnitudes, and the a_i and b_i coefficients represent respectively the slopes and zero points of the different versions of the SB relation. The particular expression of the SB relation $F_V(V - R)$ is also known as the Barnes-Evans (B-E) relation, and is historically the first version to have been calibrated empirically ([3]). However, the relatively large intrinsic dispersion of the visible B-E relation has led to prefer its infrared counterparts, in particular those based on the K band magnitudes ($\lambda = 2.0 - 2.4 \ \mu$m), as infrared wavelengths are less affected by interstellar extinction. The surface brightness F_λ is given by the following expression ([19]) :

$$F_\lambda = 4.2207 - 0.1 \, m_{\lambda_0} - 0.5 \, \log \theta_{\mathrm{LD}} \tag{4}$$

where θ_{LD} is the limb darkened angular diameter, i.e. the angular size of the stellar photosphere.

The linear expressions of the SB can be inverted easily to predict angular diameters, and give linear relations such as:

$$\log \theta_{\mathrm{LD}} = c_1 \, (V - K) + d_1 - 0.2 \, V \tag{5}$$

for the $F_V(V - K)$ inversion. We have in this example:

$$c_1 = -2 \, a_1 \tag{6}$$

$$d_1 = 2 \, (4.2207 - b_1) \tag{7}$$

In the present paper, we will refer to both the direct and inverse relations as "SB relations".

2.2. Selected measurement sample

2.2.1. Angular diameters

Over the past two years, sixteen new angular diameter measurements of nearby Main Sequence and subgiant stars were obtained with the VLT Interferometer ([21],[22],[23]) equipped with the fiber-based beam combiner VINCI ([27],[28]). To complement this sample, we have searched the literature, and added to our list the measurements related to the stars of luminosity classes IV and V. Most of the visible and infrared interferometers are represented in our sample, with measurements from the NII (*Narrabri Intensity Interferometer*[24]), the Mk III[48] , the PTI (*Palomar Testbed Interferometer*[12]) and the NPOI (*Navy Prototype Optical Interferometer*[2]). Our findings originally included a few lunar occultation measurements, but they were rejected as they were related to variable or multiple stars, or their precision was not sufficient to give them any weight in the fitting process.

In order to obtain a consistent sample of limb darkened (LD) angular diameters, we have retained solely the uniform disk (UD) values from the literature. The conversion of these model-independent measurements to LD values was achieved using the linear LD coefficients u from Claret ([10]), and the conversion formula from ([25]). These coefficients are broadband, single-parameter approximations of the Kurucz ([33]) model atmospheres. They are tabulated for a grid of temperatures, metallicities and surface gravities and we have chosen the closest models to the physical properties of the stars. We have considered a uniform microturbulent velocity of $2 \, \mathrm{km.s}^{-1}$ for all stars. This single source for limb darkening corrections ensures the consistency of our final sample.

2.2.2. Photometry

All the apparent magnitudes that we have retained from the literature are expressed in the Johnson system. When available, we have preferentially kept the uncertainties given by the original authors, otherwise we applied arbitrarily a conservative error bar. The U band magnitudes were obtained from ([39]) and ([38]). We adopted a ± 0.02 error for these values. The B, V, R and I bands were obtained from several online catalogues available through VIZIER[45] , and we also adopted a ± 0.02 uncertainty. For the J to L infrared bands, references are not so easy to find, as many bright stars are unfortunately absent from the recent infrared surveys, like 2MASS[13] or DENIS[20] . We have relied on the VIZIER database to obtain the infrared magnitudes of our sample of stars. In some cases, the references we used are 30 years old, but many of them have small and reliable uncertainties.

2.2.3. Final sample

We report in Table 1 the complete set of measurements that we have considered for our fit. In this table, the angular diameters θ_{UD} (uniform disk) and θ_{LD} (limb-darkened disk) are expressed in milliarcseconds (mas). The limb darkening conversion coefficient $k = \theta_{\mathrm{LD}}/\theta_{\mathrm{UD}}$ was computed for each star based on the tables of Claret ([10]). When a physical parameter was not available in the literature, it has been estimated approximately, and appears in *italic* characters. The observation wavelength λ is given either as the name of the photometric band (V, H, K) or the actual wavelength in μm. The error bar on the angular diameter of the Sun (G2V) has been set arbitrarily to $\pm 0.1\%$. The interferometer used for each measurement is indicated in the "Instr." column.

2.3. Surface brightness relations fitting

For each angular diameter measurement θ_{LD}, and based on the observed apparent magnitudes m_λ, we have computed the surface brightness F_λ in all the available bands, using the definition of Eq. 4. The resulting F_λ values were then fitted relatively to the colors $(C_0 - C_1)$, using a linear model. This fit was achieved using a classical χ^2 minimization taking into account the errors on both the colors and F_λ. The $1\,\sigma$ errors σ_a and σ_b are subsequently estimated from the best fit values a and b by solving numerically the expression:

$$\chi^2_{\mathrm{red}}(a + \sigma_a, b + \sigma_b) = \chi^2_{\mathrm{red}}(a, b) + 1. \tag{8}$$

From there, we can invert these relations easily to obtain their angular diameter counterparts:

$$\log \theta_{\mathrm{LD}} = c\,(C_0 - C_1) + d - 0.2\,C_0 \tag{9}$$

The slopes and zero points are computed from the (a, b) pairs through:

$$c = -2\,a, \quad \sigma_c = 2\,\sigma_a \tag{10}$$

$$d = 2\,(4.2207 - b), \quad \sigma_d = 2\,\sigma_b \tag{11}$$

2.4. Least dispersed relations

The SB relations take the form:

$$\log \theta_{\mathrm{LD}}(C_0, C_1) = c_\lambda(C_0 - C_1) + d_\lambda - 0.2\,C_0 \tag{12}$$

where C_0 and C_1 are any two distinct colors of the Johnson system. The best relations based on the K band, showing residual dispersions **below 1%** on the angular diameter θ_{LD}, are the following:

$$\log \theta_{\mathrm{LD}} = 0.0535 \pm 0.0006\,(B - K) + 0.5159 \pm 0.0016 - 0.2\,K \tag{13}$$

$$\log \theta_{\mathrm{LD}} = 0.0755 \pm 0.0008\,(V - K) + 0.5170 \pm 0.0017 - 0.2\,K. \tag{14}$$

and the best relations for the L band are:

$$\log \theta_{\mathrm{LD}} = 0.0412 \pm 0.0005\,(U - L) + 0.5167 \pm 0.0017 - 0.2\,L \tag{15}$$

$$\log \theta_{\mathrm{LD}} = 0.0502 \pm 0.0006\,(B - L) + 0.5133 \pm 0.0018 - 0.2\,L \tag{16}$$

Table 1. Angular diameters of dwarf stars (luminosity class V, upper part) and subgiants (class IV, lower part) measured by long-baseline interferometry (apart from the Sun). They are expressed in mas, and T_{eff} is in K. "Ref.$_1$" designates the reference used for T_{eff}, $\log g$ and [Fe/H]. When unavailable, the metallicity has been set arbitrarily to the solar value. "Ref.$_2$" designates the reference used for each angular diameter measurement (expressed in mas). The error bars are given in superscript close to each value.

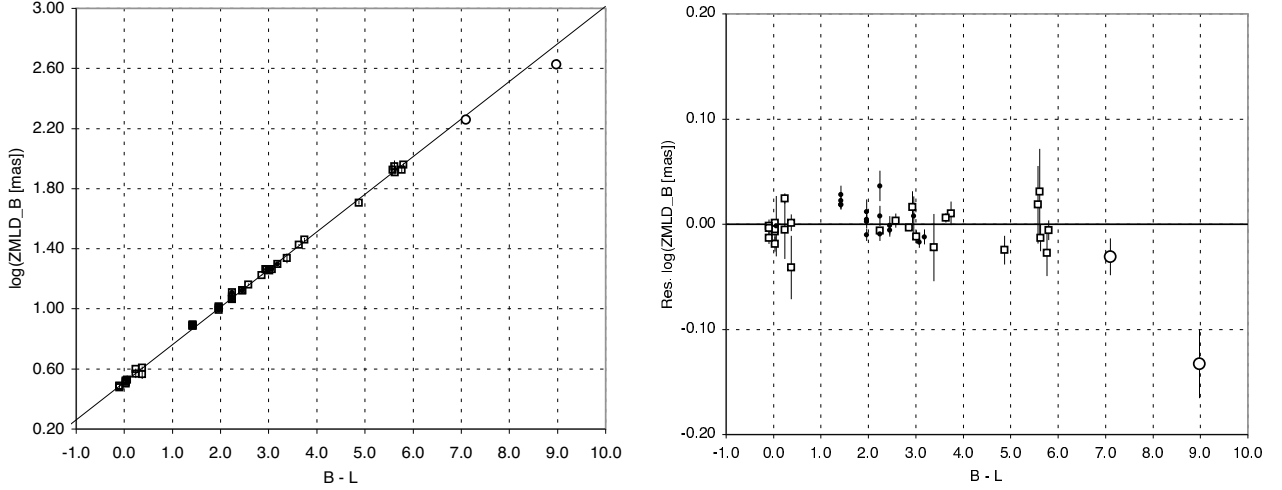| Star	Spect.	Ref.$_1$	T_{eff}	$\log g$	[Fe/H]	Instr.	Ref.$_2$	λ	θ_{UD}	k	θ_{LD}
α Lyr	A0V	(^{8},^{51})	9522	3.98	-0.33	PTI	(^{9})	K	$3.24^{0.01}$	1.012	$3.28^{0.01}$
α Lyr	A0V	(^{8},^{51})	9522	3.98	-0.33	NII	(^{26})	V	$3.08^{0.07}$	1.046	$3.22^{0.07}$
α Lyr	A0V	(^{8},^{51})	9522	3.98	-0.33	Mk III	(^{42})	0.8	$3.15^{0.03}$	1.028	$3.24^{0.03}$
α Lyr	A0V	(^{8},^{51})	9522	3.98	-0.33	Mk III	(^{42})	0.55	$3.00^{0.05}$	1.046	$3.13^{0.05}$
α CMa A	A1V	(^{6})	9800	4.30	0.40	NII	(^{14})	V	$5.60^{0.07}$	1.045	$5.85^{0.07}$
α CMa A	A1V	(^{6})	9800	4.30	0.40	VLTI	(^{29})	K	$5.94^{0.02}$	1.012	$6.01^{0.02}$
α CMa A	A1V	(^{6})	9800	4.30	0.40	Mk III	(^{42})	0.8	$5.82^{0.11}$	1.027	$5.98^{0.11}$
β Leo	A3V	(^{18})	8570	4.26	0.20	VLTI	(^{15})	K	$1.43^{0.03}$	1.015	$1.45^{0.03}$
β Leo	A3V	(^{18})	8570	4.26	0.20	NII	(^{26})	V	$1.25^{0.09}$	1.052	$1.31^{0.09}$
α PsA	A3V	(^{18})	8760	4.22	0.43	NII	(^{26})	V	$1.98^{0.13}$	1.050	$2.08^{0.14}$
α PsA	A3V	(^{18})	8760	4.22	0.43	VLTI	(^{15})	K	$2.20^{0.02}$	1.014	$2.23^{0.02}$
α Cen A	G2V	(^{40})	5790	4.32	0.20	VLTI	(^{30})	K	$8.31^{0.02}$	1.024	$8.51^{0.02}$
τ Cet	G8V	(^{15})	5400	4.55	-0.45	VLTI	(^{15})	K	$2.03^{0.03}$	1.024	$2.08^{0.03}$
GJ 166 A	K1V	(^{8})	5073	4.19	-0.31	VLTI	(^{50})	K	$1.60^{0.06}$	1.029	$1.65^{0.06}$
α Cen B	K1V	(^{40})	5260	4.51	0.23	VLTI	(^{30})	K	$5.86^{0.03}$	1.026	$6.01^{0.03}$
ϵ Eri	K2V	(^{8})	5052	4.57	-0.15	VLTI	(^{15})	K	$2.09^{0.03}$	1.027	$2.15^{0.03}$
GJ 105 A	K3V	(^{8})	4718	4.50	-0.07	PTI	(^{34})	H, K	$0.91^{0.07}$	1.032	$0.94^{0.07}$
GJ 570 A	K4V	(^{8})	4533	4.79	0.02	VLTI	(^{50})	K	$1.19^{0.03}$	1.030	$1.23^{0.03}$
GJ 845 A	K4.5V	(^{6})	4500	4.50	-0.10	VLTI	(^{50})	K	$1.84^{0.02}$	1.030	$1.89^{0.02}$
GJ 380	K7V	(^{8})	3861	4.68	-0.93	PTI	(^{34})	H, K	$1.27^{0.04}$	1.018	$1.29^{0.04}$
GJ 191	M1V	(^{6})	3524	4.87	-0.50	VLTI	(^{49})	K	$0.68^{0.06}$	1.016	$0.69^{0.06}$
GJ 887	M0.5V	(^{49})	3645	4.80	*0.00*	VLTI	(^{49})	K	$1.37^{0.04}$	1.018	$1.39^{0.04}$
GJ 205	M1.5V	(^{6})	3626	4.80	0.60	VLTI	(^{49})	K	$1.12^{0.11}$	1.020	$1.15^{0.11}$
GJ 15 A	M2V	(^{8})	3721	5.00	-1.40	PTI	(^{34})	H, K	$0.98^{0.05}$	1.017	$1.00^{0.05}$
GJ 411	M1.5V	(^{7})	3620	4.90	-0.20	PTI	(^{34})	H, K	$1.41^{0.03}$	1.019	$1.44^{0.03}$
GJ 699	M4Ve	(^{8})	3201	5.00	-0.90	PTI	(^{34})	H, K	$0.99^{0.04}$	1.018	$1.00^{0.04}$
Proxima	M5.5V	(^{49})	3006	5.19	*0.00*	VLTI	(^{49})	K	$1.02^{0.08}$	1.030	$1.05^{0.08}$
γ Gem	A0IV	(^{6})	9260	3.60	-0.12	NII	(^{26})	V	$1.32^{0.09}$	1.047	$1.38^{0.09}$
α CMi A	F5IV-V	(^{1})	6530	3.96	-0.05	VLTI	(^{31})	K	$5.38^{0.05}$	1.019	$5.48^{0.05}$
α CMi A	F5IV-V	(^{1})	6530	3.96	-0.05	NPOI	(^{44})	V	$5.19^{0.04}$	1.057	$5.49^{0.04}$
α CMi A	F5IV-V	(^{1})	6530	3.96	-0.05	Mk III	(^{42})	0.8	$5.32^{0.08}$	1.039	$5.53^{0.08}$
α CMi A	F5IV-V	(^{1})	6530	3.96	-0.05	Mk III	(^{42})	0.55	$5.30^{0.11}$	1.057	$5.60^{0.11}$
η Boo	G0IV	(^{8})	6003	3.62	0.25	VLTI	(^{52})	K	$2.15^{0.03}$	1.022	$2.20^{0.03}$
η Boo	G0IV	(^{8})	6003	3.62	0.25	Mk III	(^{42})	0.8	$2.18^{0.02}$	1.044	$2.27^{0.03}$
η Boo	G0IV	(^{8})	6003	3.62	0.25	Mk III	(^{42})	0.55	$2.13^{0.03}$	1.063	$2.26^{0.03}$
η Boo	G0IV	(^{8})	6003	3.62	0.25	NPOI	(^{44})	V	$2.17^{0.06}$	1.064	$2.31^{0.06}$
ζ Her A	G0IV	(^{41})	5820	3.85	0.04	Mk III	(^{42})	0.8	$2.26^{0.05}$	1.045	$2.36^{0.05}$
ζ Her A	G0IV	(^{41})	5820	3.85	0.04	Mk III	(^{42})	0.55	$2.13^{0.03}$	1.065	$2.27^{0.03}$
ζ Her A	G0IV	(^{41})	5820	3.85	0.04	NPOI	(^{44})	V	$2.37^{0.08}$	1.065	$2.52^{0.09}$
μ Her	G5IV	(^{8})	5411	3.87	0.16	Mk III	(^{42})	0.8	$1.86^{0.04}$	1.049	$1.95^{0.04}$
μ Her	G5IV	(^{8})	5411	3.87	0.16	Mk III	(^{42})	0.55	$1.81^{0.03}$	1.070	$1.93^{0.03}$
β Aql	G8IV	(^{8})	5041	3.04	-0.04	NPOI	(^{43})	V	$2.07^{0.09}$	1.075	$2.23^{0.10}$
η Cep	K0IV	(^{8})	5013	3.19	-0.19	NPOI	(^{43})	V	$2.51^{0.04}$	1.064	$2.67^{0.04}$
δ Eri	K0IV	(^{8})	4884	3.40	-0.11	VLTI	(^{52})	K	$2.33^{0.03}$	1.027	$2.39^{0.03}$

Figure 1. Linear fit of the surface brightness relation $\log \mathrm{ZMLD}_B(B - L)$ (upper part), and the corresponding residuals (lower part). The intrinsic dispersion of the relation is ± 0.004 on $\log \mathrm{ZMLD}$, equivalent to a systematic error of less than 1% on the predicted angular diameters. The open circles designate GJ 699 and *Proxima*, that were excluded from the fitting procedure.

$$\log \theta_{\mathrm{LD}} = 0.0701 \pm 0.0008\,(V - L) + 0.5139 \pm 0.0019 - 0.2\,L \tag{17}$$

$$\log \theta_{\mathrm{LD}} = 0.1075 \pm 0.0014\,(R - L) + 0.5128 \pm 0.0021 - 0.2\,L. \tag{18}$$

The Zero Magnitude Limb Darkened disk angular diameter (ZMLD) corresponds to the angular size of the star if its apparent magnitude was zero. Late spectral types ZMLD are larger than early type stars, as their surface brightness is lower. These expressions are valid at least over the range of colors defined by our sample (Table 1). In terms of spectral types, the angular diameter predictions can be considered reliable between A0 and M2 for dwarfs, and between A0 and K0 for subgiants. There are indications (Fig. 1) that the infrared relations are mostly valid down to the spectral type M4V of GJ 699, but show some discrepancy for the M5.5V star *Proxima*. The established relations are likely to be valid also for subgiants of spectral types later than K0IV, but this cannot be verified based on our sample. It should be stressed that they are applicable only to single stars, and the presence of a non resolved stellar companion contributing for a significant fraction of the measured flux will bias the predicted angular diameters. As more than half of the Main Sequence stars are binary or multiple stars, care should be taken in the application of these relations.

3. PROPERTIES OF DWARF STARS AS CALIBRATORS

3.1. The need for small and nearby calibrators

Interferometric observations are generally based on interspersed observations of a scientific target and a calibrator. The angular size of the calibrator is supposed to be known *a priori*, and the observed fringe contrast is used to estimate the instrumental transfer function (also called system visibility). The catalogue of calibrators assembled by Cohen et al. ([11]), customized to interferometry by Bordé et al. ([5]), consists mainly of K giants with angular diameters of about 2 mas. While this size is well adapted to short baseline observations (up to a few tens of meters in the infrared), these stars are too large angularly to serve as calibrators for the hectometric baselines of the VLTI, the CHARA array[36] or the NPOI[2] . In addition, it is foreseen to implement on the VLTI shorter wavelengths than the K band currently accessible with VINCI. For instance, the AMBER instrument[46] will allow observations in the J band. The two fold increase in angular resolution will naturally require significantly smaller calibrators than the Cohen et al. ([11]) catalogue. Mérand et al. ([37]) have prepared an extension of this catalogue to smaller giants, that are adapted to 200 m baselines.
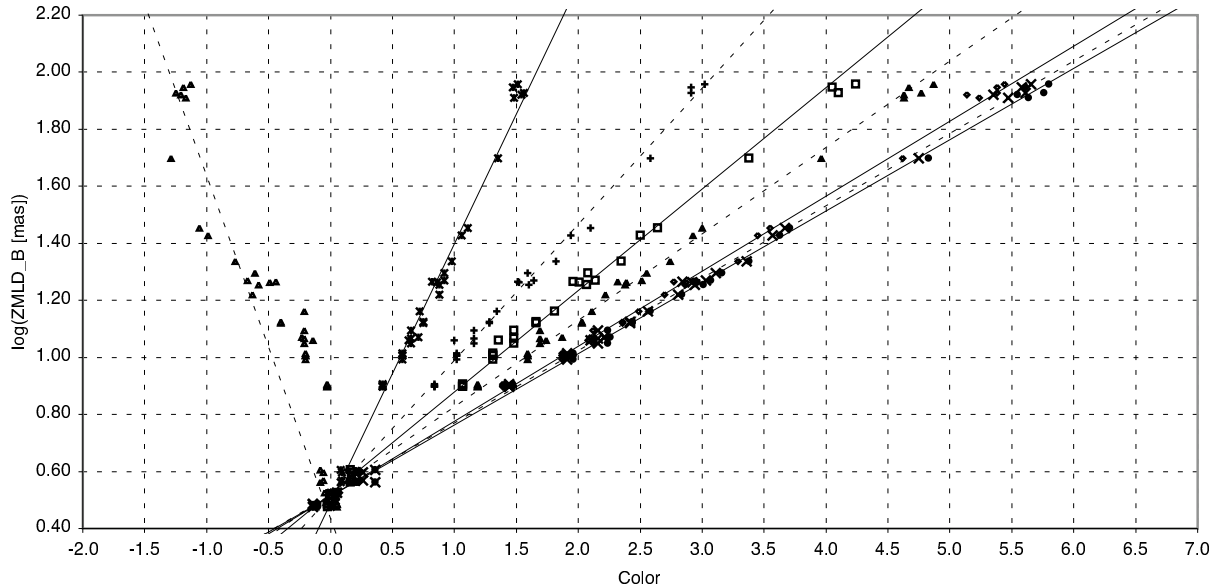
Figure 2. Johnson B band ZMLD$_B$ relations as a function of colors. The error bars have been omitted for clarity, and the fitted models are represented alternatively as solid and dashed lines. From left to right, using the colors: $(B - U)$, $(B - V)$, $(B - R)$, $(B - I)$, $(B - J)$, $(B - H)$, $(B - K)$, $(B - L)$. A clear non linearity is visible on the $(B - U)$ based relation.

A fundamental problem with distant stars is that the reddening corrections are uncertain. This means that it is highly desirable to use nearby stars as calibrators, located within a few tens of parsecs. In this respect, giant stars are not well suited due to their large linear dimensions, but dwarfs and subgiants are ideally adapted to provide small and well-defined calibrators.

Another advantage of Main Sequence stars is that their strong surface gravity results in a compact atmosphere and a well-defined photosphere. Their disk appears sharper than the giants, for which the precise definition of the limb darkened disk angular diameter at a level of less than 1 % can be difficult, in particular for the later spectral types. As an example, a discussion about the M4III giant ψ Phe can be found in.[53]

3.2. Sources of uncertainty on the predicted diameters

Several observational and astrophysical sources of uncertainty add up to create the total error bar on the predicted angular diameters:

- *intrinsic dispersion of the empirical relation:* as discussed above, the best relations have intrinsic dispersions below 1%. It should be stressed that their predictions cannot be averaged to reduce this systematic uncertainty. However, the predictions from independent colors (such as $V - K$ and $B - L$) can be averaged to reduce the statistical uncertainty on the predictions due to the error bars on the photometric measurements. In this process, the systematic uncertainties of each relation *cannot* be reduced and have to be carefully taken into account. This is essential as the calibrations have been obtained for all colors from the same sample of stars, and the resulting systematic errors are therefore highly correlated.

- *uncertainties on the apparent magnitudes:* combining the high precision magnitudes available in the visible with the infrared magnitudes produced by the 2MASS and DENIS surveys should enable to retrieve the visible-infrared color indices with a precision better than ± 0.02 mag. However, we would like to stress that the uncertainty on the apparent magnitude measurements can easily be the largest contributor to the
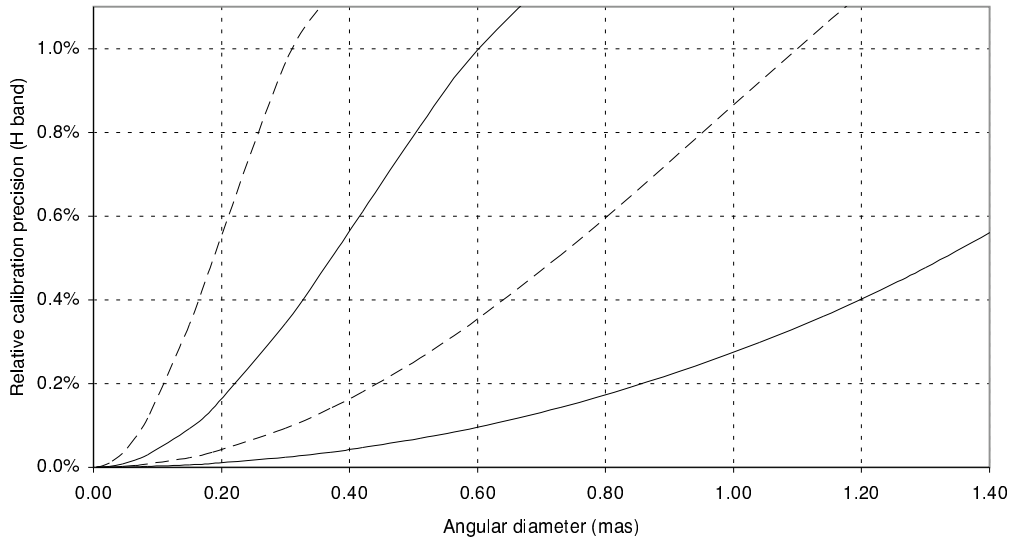
Figure 3. Precision achievable on the measurement of the interferometric efficiency as a function of the angular diameter of the calibrator, predicted using the $(B, B - L)$ SB relation ($\leq 1.0\%$ dispersion). From left to right, the curves refer to baselines of 800, 400, 200 and 100 m, in the H band.

predicted angular diameter error bars. The true error bars on the photometric measurements have to be estimated accurately in order to obtain reasonable uncertainties on the predicted angular sizes.

- *interstellar extinction and circumstellar matter:* for the sample of nearby stars that was considered for our fits, the interstellar extinction is negligible: apart from γ Gem at 32 pc, all stars are located closer than 15 pc. However, our SB relations are strictly valid only for extinction corrected magnitudes. The uncertainty on the assumed color excess $E(B - V)$ (for instance) will translate into an additional uncertainty on the dereddened magnitudes. The presence of a significant ammount of circumstellar matter around the star will also affect its spectral properties, and can be difficult to detect.

3.3. Calibration precision vs. brightness

It is possible to estimate the maximum angular size of calibrator stars in order to obtain a given relative precision on the calibration of the interferometric efficiency. Fig. 3 shows the achievable precision on the interferometric efficiency using the $(B, B - L)$ relation determined in Sect. 2.4 ($\sigma \leq 1.0\%$), as a function of the angular diameter of the calibrator star, for four different baselines (100, 200, 400 and 800 m), in the H band. These baselines are representative of the existing or foreseen interferometers (Keck, PTI, VLTI, CHARA, NPOI and OHANA, sorted by increasing maximum baseline). The horizontal scale of Fig. 3 can be adapted for other wavelengths or other baselines by scaling it linearly while maintaining constant the B/λ ratio.

If we now set a limit of 0.5% on the acceptable systematic uncertainty on the interferometric efficiency, we can compute the apparent magnitude of the Main Sequence calibrators that should be used as a function of their color. The result is presented on Fig. 4 as a function of the $B - H$ color, for different baseline lengths and interferometric observations in the H band. From this figure, it can be concluded that suitable calibrators for extremely long baseline observations will have to be faint. Let us consider the example of the OHANA interferometer (original idea proposed by Mariotti et al.[35]), whose longest foreseen baseline is 800 m. The H band magnitude of the calibrators necessary to obtain a relative systematic visibility error of 0.5% will be between $m_H = 6$ and 8, depending on the spectral type. This is rather faint, even for large aperture light collectors, but is feasible with OHANA. As an alternative, it is possible to build (through time consuming observations) a
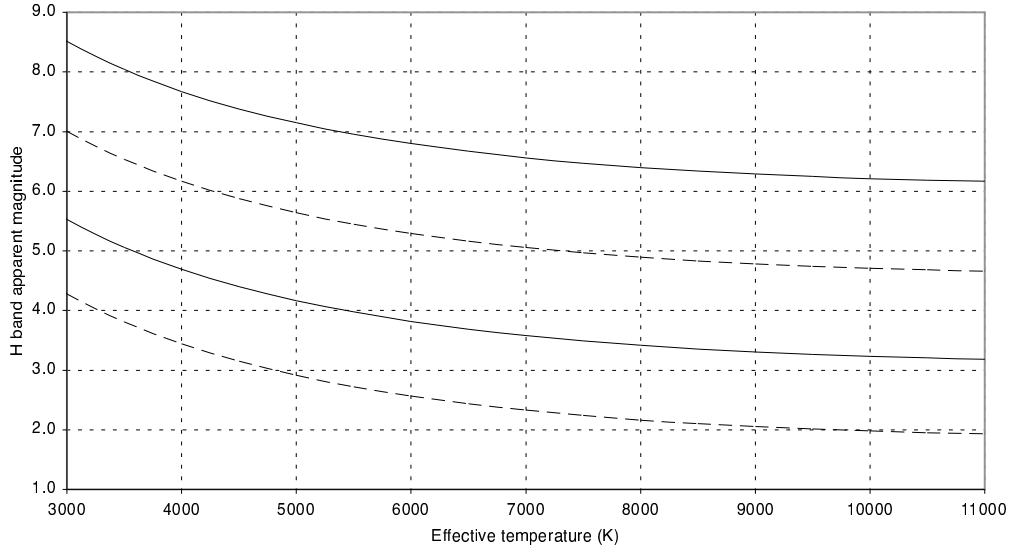
Figure 4. Apparent magnitude in the H band of the calibrators suitable to obtain a relative precision of 0.5% on the calibration of the interferometric efficiency, as a function of the $B - H$ color. From top to bottom, the curves refer to baselines of 800, 400, 200 and 100 m, in the H band.

secondary network of brighter and larger calibrators based on the small angular diameter ones, but there will always be a limitation attached to the fact that calibrators have to be observed in the first lobe of their visibility function. For OHANA, this sets a hard limit of $\simeq 0.5$ mas to the calibrator angular size, and even ≤ 0.4 mas to obtain a visibility of at least 0.3. This corresponds to apparent magnitudes of $m_H = 5$ to 7 in the H band, one magnitude brighter than the primary network. For the longest baseline of the VLTI (200 m), calibrator magnitudes between $m_H = 3$ and 5 will be sufficient, clearly in the accessible domain of the AMBER beam combiner[46] with the 1.8 m Auxiliary Telescopes.[32] The creation of a secondary network of calibrators should therefore not be necessary.

It should be stressed that the present conclusions regarding magnitudes are not limited to dwarf stars, as giants and supergiants follow comparable surface brightness relations. This means that the magnitude ranges defined above will be almost the same for other luminosity classes. A decisive advantage of dwarfs is that for the same apparent magnitude, they will be much closer than the more luminous classes, and therefore significantly less affected by interstellar extinction.

3.4. Metallicity

A possible source of natural dispersion of the SB relations is the presence of deep absorption lines in the spectrum of the stars. This effect is stronger for stars that have a high metal content. However, as shown on Fig. 5, no correlation could be evidenced between the residuals of the least dispersed relation $\theta_{\mathrm{LD}}(L, B - L)$ and the metallicity [Fe/H]. This is an indication that our SB relations are valid at least for metallicities between -0.5 and $+0.5$ dex, and probably also for lower values. The two metal-deficient stars of Fig. 5 are GJ 15 A ([Fe/H]$= -1.40$ dex) and GJ 699 ([Fe/H]$= -0.90$ dex, not included in our fits). For typical stars of the solar neighborhood, our relations are thus always applicable.

3.5. Multiplicity rate and stability

The multiplicity rate of AFGKM dwarfs is currently not known with precision, but probably in the 50% range ([17]). The presence of a second star in the same interferometric field as the primary target can lead to a significant
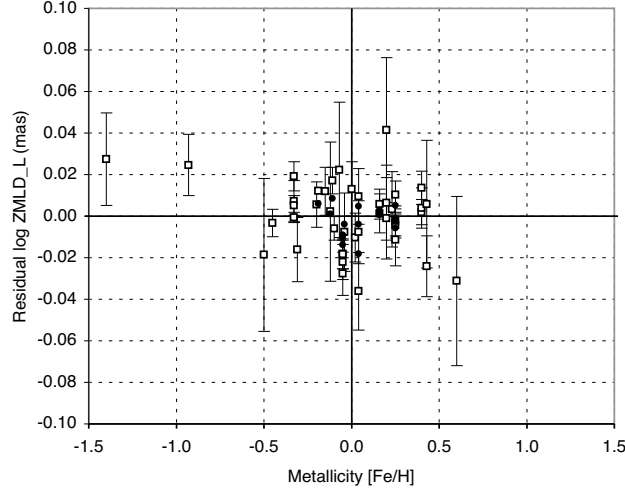
Figure 5. Residuals of the fit of $\mathrm{ZMLD}_L(L, B - L)$ as a function of the metallicity [Fe/H] of the star. Dwarfs are represented by open squares, and subgiants by solid dots. No correlation is visible among the stars of our sample.

bias on the visibility, and thus on the estimated interferometric transfer function. This means that a significant fraction of the nearby stars may not be suitable to be used as calibrators.

However, this potential problem is considerably less critical for nearby dwarfs as it is for more distant stars, for two reasons:

- Medium to long period companions are separated angularly from the primary star, and are thus likely to be detected using direct imaging techniques.

- Nearby massive companions contributing for a significant fraction of the flux of the pair are easily identified using spectroscopy, either through their flux contribution or the induced radial velocity variations. Very low mass companions (planetary mass bodies for instance) usually do not contribute for a significant fraction of the total flux.

Overall, dwarf star companions are therefore easy to identify, thanks to the smaller distances involved, especially compared to giant and supergiant stars of comparable apparent magnitudes.

3.6. Star counts

A query of the Hipparcos catalogue[47] returns a total of about 500 dwarfs and subgiants within 20 pc of the Sun, more than 1200 within 30 pc, and 2200 within 40 pc. Due to the limiting magnitude of this catalogue ($\simeq 11$ in V), many K and most of the M dwarfs are absent from this count, while still being within the observable domain of the large infrared interferometers. Rejecting the multiple objects from this count still leads to a number of several hundred dwarfs and subgiants, a sufficient group to provide a uniform sky coverage. As we are considering nearby stars, the high galactic latitudes are well represented, as the galactic plane.

4. CONCLUSION

The laws that we established between the angular size and broadband colors are strictly empirical. Our best relations present a very small intrinsic dispersion, down to less than 1 %. They can be used to predict the angular sizes of A0–M2 dwarfs and A0–K0 subgiants from simple, readily available broadband photometry. Several large catalogues (2MASS, DENIS,...) provide high precision magnitudes of these stars in the infrared. From the cross-comparison of these sources, the SB relations presented in the present paper make it possible

to assemble a catalogue of calibrators for interferometry that will practically not be affected by interstellar extinction, multiplicity or circumstellar material biases. These resulting angular diameter predictions will provide a reliable basis for the calibration of long baseline interferometric observations.

ACKNOWLEDGMENTS

REFERENCES

1. Allende Prieto, C., Asplund, M., Garcia Lòpez, R. J., & Lambert, D. L. 2002, *Astrophys. Journal*, **567**, 544
2. Armstrong, J. T., Mozurkewich, D., Rickard, L. J., et al. 1998, *Astrophys. Journal*, **496**, 550
3. Barnes, T. G., Evans, D. S., & Parson, S. B. 1976, *Monthly Not. Roy. Astr. Society*, **174**, 503
4. Boden, A. F., Van Belle, G. T., Colavita, M. M. 1998, *Astrophys. Journal*, **504**, 39
5. Bordé, P., Coudé du Foresto, V., Chagnon, G., & Perrin, G. 2002, *Astron. Astrophys.*, **393**, 183
6. Cayrel de Strobel, G., Soubiran, C., Friel, E.D., Ralite, N., & Francois, P., 1997, *Astron. Astrophys. Suppl.*, **124**, 299
7. Cayrel de Strobel G., Soubiran C., & Ralite N. 2001, *Astron. Astrophys.*, **373**, 159
8. Cenarro, A. J., Cardiel, N., Gorgas, J., et al. 2001, *Monthly Not. Roy. Astr. Society*, **326**, 959
9. Ciardi, D. R., Van Belle, G. T., Akeson, R. L., et al. 2001, *Astrophys. Journal*, **559**, 1147
10. Claret, A. 2000, *Astron. Astrophys.*, **363**, 1081
11. Cohen, M., Walker, R. G., Carter, B., et al. 1999, *Astronom. Journal*, **117**, 1864
12. Colavita, M. M., Wallace, J. K., Hines, B. E., et al. 1999, *Astrophys. Journal*, **510**, 505
13. Cutri, R. M., Skrutskie, M. F., Van Dyk, S., et al. 2003, Univ. of Massachusetts and IPAC, http://www.ipac.caltech.edu/2mass.
14. Davis, J., & Tango, W. J. 1986, *Nature*, **323**, 234
15. Di Folco, E., Thévenin, F., Kervella, P., et al. 2004, *in prep.*
16. Ducati, J. R. 2002, *NASA Ref. Pub.* 1294
17. Duquennoy, A., & Mayor, M. 1991, *Astron. Astrophys.*, **248**, 485
18. Erspamer, D., & North, P. 2003, *Astron. Astrophys.*, **398**, 1121
19. Fouqué, P., & Gieren, W. P. 1997, *Astron. Astrophys.*, **320**, 799
20. Fouqué, P., Chevallier, L., Cohen, M., et al. 2000, *Astron. Astrophys. Suppl.*, **141**, 313
21. Glindemann, A., Abuter, R., Carbognani, F., et al. 2000, *Proc. SPIE*, **4006**, 2
22. Glindemann, A., Argomedo, J., Amestica, R., et al. 2003a, *Proc. SPIE*, **4838**, 89
23. Glindemann, A., Argomedo, J., Amestica, R., et al. 2003b, *Astrophys. and Space Sci.*, **286**, 1
24. Hanbury Brown, R., Davis, J., Allen, L. R. 1967, *Monthly Not. Roy. Astr. Society*, **137**, 375
25. Hanbury Brown, R., Davis, J., Lake, J. W., & Thompson, R. J. 1974, *Monthly Not. Roy. Astr. Society*, **167**, 475
26. Hanbury Brown, R., Davis, J., & Allen, L. R. 1974, *Monthly Not. Roy. Astr. Society*, **167**, 121
27. Kervella, P., Coudé du Foresto, V., Glindemann, A., Hofmann, R. 2000, *Proc. SPIE*, **4006**, 31
28. Kervella, P., Gitton, Ph., Ségransan, D., et al. 2003, *Proc. SPIE*, **4838**, 858
29. Kervella, P., Thévenin F., Morel P., Bordé, P., & Di Folco, E. 2003, *Astron. Astrophys.*, **408**, 681
30. Kervella, P., Thévenin, F., Ségransan, D., et al. 2003, *Astron. Astrophys.*, **404**, 1087
31. Kervella, P., Thévenin F., Morel P., et al. 2004, *Astron. Astrophys.*, **413**, 251
32. Koehler, B., Flebus, C., Dierickx, P., et al. 2002, *ESO Messenger*, **110**, 21
33. Kurucz, R. L. 1992, IAU Symp. 149: The Stellar Populations of Galaxies, **149**, 225
34. Lane, B. F., Boden, A. F., & Kulkarni, S. R., 2001, *Astrophys. Journal*, **551**, L81
35. Mariotti, J.-M., Coudé du Foresto, V., Perrin, G., Peiqian Zhao, & Léna, P., 1996, *Astron. Astrophys. Suppl.*, **116**, 381
36. McAlister, H. A., Bagnuolo, W. G., ten Brummelaar, T. A., et al. 2000, *Proc. SPIE*, **4006**, 465

37. Mérand, A., Bordé, P., & Coudé du Foresto, V., *these proceedings*

38. Mermilliod J.-C. 1986, Catalogue of Eggen's UBV data (unpublished, available through SIMBAD)

39. Morel, M., & Magnenat, P. 1978, *Astron. Astrophys. Suppl.*, **34**, 477

40. Morel, P., Provost, J., Lebreton, Y., Thévenin, F., & Berthomieu, G. 2000, *Astron. Astrophys.*, **363**, 675

41. Morel, P., Berthomieu, G., Provost, J., & Thévenin, F. 2001, *Astron. Astrophys.*, **379**, 245

42. Mozurkewich, D., Armstrong, J. T., Hindsley, R. B., et al. 2003, *Astronom. Journal*, **126**, 2502

43. Nordgren, T. E., Germain, M. E., Benson, J. A., et al. 1999, *Astronom. Journal*, **118**, 3032

44. Nordgren, T. E., Sudol, J. J., & Mozurkewich, D. 2001, *Astronom. Journal*, **122**, 2707

45. Ochsenbein, F., Bauer, P., Marcout, J. 2000, *Astron. Astrophys. Suppl.*, **143**, 221

46. Petrov, R., Malbet, F., Richichi, A., et al. 2000, *Proc. SPIE*, **4006**, 68

47. Perryman, M. A. C., Lindegren, L., Kovalevsky, J., et al., *The Hipparcos Catalogue*, 1997, *Astron. Astrophys.*, **323**, 49

48. Shao, M., Colavita, M. M., Hines, B. E., et al. 1988, *Astrophys. Journal*, **327**, 905

49. Ségransan, D., Kervella, P., Forveille, T., Queloz, D. 2003, *Astron. Astrophys.*, **397**, L5

50. Ségransan, D., Kervella, P., Forveille, T., Queloz, D. 2004, *in prep.*

51. Thévenin F., & Idiart, T. P. 1999, *Astrophys. Journal*, **521**, 753

52. Thévenin, F., Kervella, P., et al., 2004, *in prep*

53. Wittkowski, M., Aufdenberg, J. P., & Kervella, P. 2004, *Astron. Astrophys.*, **413**, 711